Cite This: ACS Appl. Mater. Interfaces 2017, 9, 40369-40377

Evaluation of Removal Mechanisms in a Graphene Oxide-Coated Ceramic Ultrafiltration Membrane for Retention of Natural Organic Matter, Pharmaceuticals, and Inorganic Salts

Kyoung Hoon Chu,[†] Mahdi Fathizadeh,[‡] Miao Yu,^{‡,§} Joseph R. V. Flora,[†] Am Jang, Min Jang, Min Park, Sung Soo Yoo, Namguk Her, and Yeomin Yoon*,[†]

Supporting Information



ABSTRACT: Functionalized graphene oxide (GO), derived from pure graphite via the modified Hummer method, was used to modify commercially available ceramic ultrafiltration membranes using the vacuum method. The modified ceramic membrane functionalized with GO (ceramic_{GO}) was characterized using a variety of analysis techniques and exhibited higher hydrophilicity and increased negative charge compared with the pristine ceramic membrane. Although the pure water permeability of the ceramic_{GO} membrane (14.4–58.6 L/m² h/bar) was slightly lower than that of the pristine membrane (25.1–62.7 L/m² h/bar), the removal efficiencies associated with hydrophobic attraction and charge effects were improved significantly after GO coating. Additionally, solute transport in the GO nanosheets of the ceramic_{GO} membrane played a vital role in the retention of target compounds: natural organic matter (NOM; humic acid and tannic acid), pharmaceuticals (ibuprofen and sulfamethoxazole), and inorganic salts (NaCl, Na2SO4, CaCl2, and CaSO4). While the retention efficiencies of NOM, pharmaceuticals, and inorganic salts in the pristine membrane were 74.6%, 15.3%, and 2.9%, respectively, these increased to 93.5%, 51.0%, and 31.4% for the ceramic_{GO} membrane. Consequently, the improved removal mechanisms of the membrane modified with functionalized GO nanosheets can provide efficient retention for water treatment under suboptimal environmental conditions of pH and ionic strength.

KEYWORDS: ceramic ultrafiltration membrane, natural organic matters, pharmaceuticals, inorganic salts, removal mechanisms

1. INTRODUCTION

Nanofiltration (NF) and ultrafiltration (UF) membrane processes have been widely employed to obtain high removal efficiencies of conventional and emerging water contaminants, including macro- and micro-organic as well as inorganic compounds. To clarify the removal mechanisms (e.g., hydrophobic adsorption, electrostatic repulsion, and size/steric exclusion) of both membrane types, previous studies have

September 19, 2017 Received: Accepted: November 6, 2017 Published: November 7, 2017



[†]Department of Civil and Environmental Engineering, University of South Carolina, Columbia, South Carolina 29208, United States

[‡]Department of Chemical Engineering, University of South Carolina, Columbia, South Carolina 29208, United States

[§]Department of Chemical and Biological Engineering, Rensselaer Polytechnic Institute, Troy, New York 12180, United States

School of Civil and Architecture Engineering, Sungkyunkwan University, 2066 Seobu-ro, Jangan-16 Gu, Suwon, Gyeonggi-do 440-746, South Korea

^LDepartment of Environmental Engineering, Kwangwoon University, 447-1 Wolgye-Dong, Nowon-Gu, Seoul, Republic of Korea

Department of Environmental Engineering, Kyungpook National University, 80 Daehak-ro, Buk-gu, Daegu 41566, South Korea

^VDepartment of Civil and Environmental Engineering, Yonsei University, 134 Shinchon-dong, Seodaemun-gu, Seoul 120-749, South

ODepartment of Civil and Environmental Engineering, Korea Army Academy at Young-Cheon, 495 Hogook-ro, Kokyungmeon, Young-Cheon, Gyeongbuk 38900, South Korea

examined the retention performance for individual or combined contaminants, such as natural organic matter (NOM), micropollutants (e.g., hormones and pharmaceuticals), and inorganic salts. 1-8 These studies have demonstrated significant correlations between membrane retention performance and molecular size/shape, speciation/charge, and hydrophobicity of the contaminants. Although the both NF and UF membranes removed relatively large organics effectively, the UF membrane exhibited substantially lower retention for smaller organics and inorganics. Specifically, the retention of neutral organic species for both membranes was attributed to size/steric exclusion effects, whereas the retention of charged organic species was in uenced by electrostatic interactions with the charged membranes. 4-6 Additionally, while the removal of pesticides for NF membrane was not significantly in uenced by the inorganic salts CaCl2 and CaSO4, the presence of humic acid (HA) and hydrophobic structures (aromatic and nonphenylic) could lead to an increase in pesticide removal rates.

To improve the retention performance of UF membranes, numerous studies have investigated the modification of membranes with nanosized materials such as titanium oxides, 8-10 carbon nanotubes, 11-13 and graphene oxides (GOs), 14-17 which may reduce pore size and increase charge effects. Recently, GO has attracted great interest as an emerging material in the fields of water treatment, due to its extraordinary transport properties, good chemical stability, and high mechanical strength/stiffness. $^{18-20}$ Along with these GO properties, various methods have been used to modify or fabricate a supported membrane, such as grafting and coating. ^{21–23} In particular, a single-atom layer of GO is expected to be formed in nanochannels and thereby determine the permeation characteristics of a coated GO membrane. These GO nanochannels feature abundant oxygen-containing functional groups, which depend on the positions of functional groups in adjacent GO layers, leading to a higher negative charge on the membrane surface and therefore enhancements in hydrophilicity, retention, and antifouling capability. To this end, many researchers in the field of water treatment are trying to evaluate the in uence of GO nanochannels on various contaminants.

Although a few studies have reported the performance of GO membranes, most of these have focused on the evaluation of the removal mechanisms of several contaminants in water with polymeric membranes (e.g., polyvinylidene uoride, polysulfone, or poly(ether sulfone)) after GO coating. For example, Han et al. 15 prepared a GO membrane supported on microporous substrates of polyvinylidene uoride for water treatment. The GO membrane exhibited high retention for organic dyes (methyl blue and direct red 81, >99%) and inorganic salts (NaCl, Na₂SO₄, MgCl, and MgSO₄, 20-60%), due to physical sieving and electrostatic interactions. Hu and Mi et al. 16 fabricated a GO membrane on a porous polysulfon substrate for the retention of organic dyes (methylene blue and Rhodamin WT) and inorganic salts (NaCl and Na₂SO₄), with retention rates of 46-95% and 6-46%, respectively. While several studies have demonstrated the separation of oil in the oil/water emulsions using GO supported on the hydrophilic ceramic membrane (hereafter referred to as the ceramic_{GO} membrane), 24,25 there is a lack of information about the retention mechanisms of other contaminants.

Previous studies have also been limited to the effects of environmental or experimental conditions, such as our previous study where we investigated the removal of NOM as a function

of pH and ionic strength using a GO membrane. 26,27 However, numerous challenges remain for the various contaminants relevant to water treatment, and to date no studies have evaluated the performance of a GO membrane for the removal of micropollutants (e.g., pharmaceuticals). As a first attempt to explore these issues, GO powders prepared in the laboratory were deposited on commercially available ceramic UF membranes with nominal molecular weight cut-offs (MWCOs) of 1, 5, and 15 kDa via a vacuum method. Then, we used various analysis techniques to characterize the physicochemical properties of prepared GO powders and the resulting ceramic_{GO} membranes. We also performed membrane retention tests for different organic and inorganic compounds of NOM, pharmaceuticals, and salts contaminants to demonstrate the removal mechanisms (i.e., size exclusion, hydrophobic adsorption, and electrostatic repulsion) of the pristine ceramic and ceramic_{GO} membranes. Finally, we assessed the retention of pharmaceuticals and inorganic salts for the ceramic_{GO} membrane under different pH and ionic strength conditions to evaluate the charge effects between the membrane and the target compounds.

2. EXPERIMENTAL SECTION

2.1. GO Preparation and Membrane Modification. To prepare GO powders in our laboratory, pure graphite, NaNO3, H2SO4, KMnO₄, H₂O₂ (30 wt %), and HCl (5%) were purchased from Sigma-Aldrich (U.S.A.). We did not perform any further purifications, because all chemicals used were of analytical reagent grade. The GO powders were synthesized from pure graphite via the modified Hummer method.²⁸ Brie y, 1 g of pure graphite and 0.5 g of NaNO₃ were placed in a ask and mixed with 75 mL of concentrated H₂SO₄ under constant stirring. After mixing for 1 h, 6 g of KMnO₄ was added to the suspension, when the temperature was maintained at less than 20 °C using an ice bath, and then mixture was stirred for 2 h. Following this, the mixture was stirred at room temperature for 18 h and then heated at 70 °C with stirring for an additional 2 h.

Next, the suspension was diluted slowly by adding 100 mL of deionized water and then heated at 90 °C under stirring for another 1 h. To ensure the completion of the reaction with KMnO₄, the suspension was further treated with deionized water (100 mL) and 30 wt % H₂O₂ (30 mL) solution. The resulting mixture was washed repeatedly under vacuum filtration with 5% HCl and distilled water until the pH of the mixture was neutral, to remove any oxidant ions and other impurities. Next, the dispersion, sonicated at a frequency of 40 Hz for 1 h (Branson 2510R-DTH), was centrifuged (Bio Lion XC-H165) at 9000 rpm for 20 min. Finally, the resulting GO dispersion was diluted with deionized water and used as a homogeneous stock GO solution. Following a method described in our previous studies, 26,27,29 we determined the concentration of the stock GO solution by ultraviolet-visible (UV-vis) spectroscopy (Shimadzu UF-

Commercially available ceramic UF membranes with different nominal MWCOs (1, 5, and 15 kDa) were purchased from Sterlitech Co. (Kent, WA, U.S.A.) and modified with the prepared GO dispersion using a vacuum method. The procedure of membrane modification is well described in our previous studies 26,27,30 and is illustrated in Figure S1. On the basis of our previous results, we used 10 nm thick ceramic_{GO} membranes. To control the thickness of the ceramic_{GO} membranes, the prepared GO suspension (12.167 g of stock GO dilute to 30 mL) was filtered using the Millipore system. After GO deposition, the membranes were rinsed with ultrapure water to remove weakly bonded or unbonded GO from the membrane surface. Finally, the $\mathsf{ceramic}_{\mathsf{GO}}$ membranes were heated at 100 $^{\circ}\mathsf{C}$ for 2 h to increase the bond strength of GO coated on the membranes, for use in subsequent experiments.

2.2. Physicochemical Characterization. The surface morphology, crystal phases, and functional groups of prepared GO powders **ACS Applied Materials & Interfaces**

Table 1. Physicochemical Properties of IBP and SMX

Pharmaceuticals	Ibuprofen (IBP)	Sulfamethoxazole (SMX)
Classification	Pain reliever	Antibiotic
Molecular weight (g/mol)	206.3	253.3
Stokes radius (nm)	0.34 ^a	0.38 ^a
pK_a	4.4 ^b –4.9 ^c	$pK_{a1}=1.7^d$, $pK_{a2}=5.6^d-5.7^e$
$\log K_{\rm OW}$	3.5°, 4.13 ^b	0.89°
Water solubility (g/L at 25 °C)	0.049 ^b	0.6 ^e
Henry's law constant (atm-m ³ /mol)	1.50×10 ⁻⁷	6.42×10 ⁻¹³
Vapor pressure (mmHg at 25°C)	1.39 × 10 ⁻⁴	6.93 × 10 ⁻⁸
Chemical structure	CH ₃ OH	H ₂ N N

aThe size of neutral pharmaceutical species was determined by the Stockes-Einstein and Wilke-Chang equations. 41 Beference 42. Reference 43. ^dReference 44. ^eReference 45.

were characterized using biological transmission electron microscopy (Bio-TEM), X-ray diffraction (XRD), and Fourier-transform infrared (FTIR). The Bio-TEM (HT-7700, Hitachi, Ltd., Japan) images of the surfaces of the GO powders were captured at low and high magnifications. The XRD diffraction patterns (D/Max-2500, Rigaku, Japan) were collected at room temperature in the range 5° with a step width of 0.02°. The FTIR spectra (Nicolet 6700, Thermo Scientific, U.S.A.) were collected in the range of 400–4000 cm⁻¹ using an attenuated total re ectance accessory. Furthermore, the characteristics of binding energies and chemical structures of the GO powders were measured by X-ray photoelectron spectroscopy (XPS) and Raman measurements. High-resolution spectra were evaluated using a K-Alpha XPS spectrometer (Thermo Fisher Scientific, U.K.), which was calibrated by setting C 1s in the rage of 278-298 eV at 24.4 W. Additionally, the inVia re ex Raman spectrometer (Renishaw, U.K.) was equipped with a cooled silicon charge coupled device detector.

To characterize pristine ceramic and ceramic_{GO} membranes, high quality field emission-scanning electron microscopy (FE-SEM, Zeiss UltraPlus, Germany) images were obtained using a low voltage of 2-5 kV, a small size of <15 mm, and a short distance of <4 mm. The hydrophilicity of each membrane was investigated using a confocal laser scanning microscope (CLSM, NanoFocus, µsurf explorer, Germany), and the resulting value of RSa or RSq was used to characterize the roughness parameter. In addition to FE-SEM and CLSM measurements, contact angle experiments were performed using a VCP Optima XE system (AST Products, Inc., U.S.A.), where water (1 μ L) was dropped onto the membrane surface. Finally, a streaming potential instrument (SurPASS, Anton Paar, Austria) was used to evaluate the zeta potential of both membranes. The electrolyte solution (i.e., 10 mM NaCl) was used in a range of pH values from 3-10 using an automated titration unit. The Fairbrother-Mastin approach was used to obtain zeta potentials from potential and pressure data.

2.3. Target Compounds and Analyses. In evaluating the removal mechanisms of size exclusion, hydrophobic adsorption, and electrostatic repulsion for the ceramic_{GO} membrane, the various target compounds should include different molecular sizes, hydrophobicity, and repulsive forces. Thus, we selected four organics (HA and tannic acid (TA) as NOM and ibuprofen (IBP) and sulfamethoxazole (SMX) as pharmaceuticals) and four inorganic salts (NaCl, Na2SO4, CaCl2,

and CaSO₄), obtained from Sigma-Aldrich (U.S.A.), as singlefeedwater solutions for the filtration experiments. Assessing the applicability of the membrane for water treatment also requires understanding the characteristics of these compounds under real-world conditions. Therefore, the feed concentrations used were based on actual water treatment processes: 10 mg/L for NOM, 10 µM for pharmaceuticals, and 1-10 mM for inorganic salts.

To achieve the desired feed concentrations of the NOM and inorganic salts, stock solutions were prepared by dissolving each compound in deionized ultrapure water, and then filtered with 0.7 and 0.45 μ m filters (Millipore Inc., U.S.A.). The feed solutions for the retention experiments were prepared by further dilution of NOM and inorganic salt stock solutions with deionized water to obtain the desired concentrations. In addition, Table 1 lists the characteristics of the selected target pharmaceuticals (IBP and SMX). Because of the low water solubility of the pharmaceuticals, IBP and SMX stock solutions were prepared in acetonitrile and kept in 40 mL amber vials equipped with screw caps. The pH was adjusted with both 0.1 M HCL and NaOH solutions and then buffered by a chemical solution of 1 mM phosphate. The conductivity was also adjusted with 0.1 M NaCl

Before the measurements, all compounds were filtered through a $0.22 \mu m$ Durapore membrane filter (Millipore Inc., U.S.A.). NOM and inorganic salts were analyzed using UV-vis spectroscopy (absorbance at 254 nm) and a conductivity meter (Accumet Excel XL30, Thermo Scientific, U.S.A), respectively. Pharmaceuticals were placed in a 2 mL amber vial and measured by high-performance liquid chromatography with UV detection, using a 5 μ m column (LiChrosper RP-18, Agilent, USA) at a ow rate of 0.75 mL/min for 23 min. The mobile phase was a 50:50 (v/v) mixture of phosphoric acid (5 mM) and acetonitrile. IBP and SMX eluted from the column at 3.8 and 21 min, respectively, with detection at 210 nm.

2.4. Membrane Retention Performance. The pure water permeability test was conducted on the pristine ceramic and ceramic_{GO} membranes in a dead-end cell filtration system (Sterlitech Corporation, U.S.A.), before the retention performance of the membranes was characterized. This system had a total volume of 300 mL and an effective membrane surface area of 14.2 cm². The stirring speed and transmembrane pressure were set to constant values of 300 rpm and 3 **ACS Applied Materials & Interfaces**

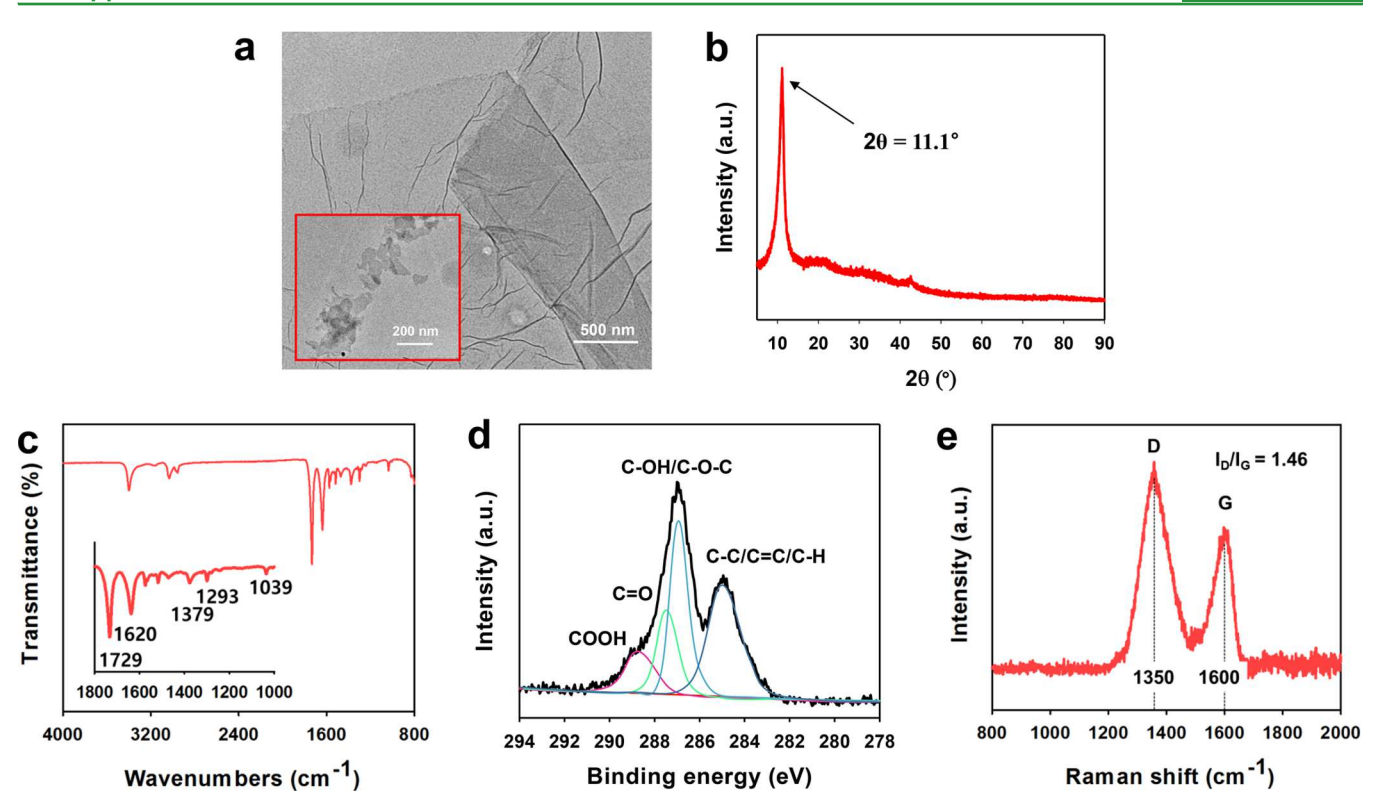


Figure 1. Physicochemical properties of prepared GO nanosheets using (a) Bio-TEM, (b) XRD, (c) FTIR, (d) XPS, and (e) Raman measurements.

bar, respectively. Following this, we conducted retention experiments on the aforementioned NOM, pharmaceuticals, and inorganic salts in the same system to demonstrate the removal mechanisms for both membranes. For the average removal efficiency determination of the target compounds, the permeate samples were collected every 30 mL until a water recovery of 90% was reached, corresponding to a volume concentration factor (VCF = $V_{\rm F}/V_{\rm R} = 1 + V_{\rm P}/V_{\rm R}$) of 10. Here, $V_{\rm F}$, $V_{\rm R}$, and $V_{\rm P}$ are defined as the volume of feed, retentate, and permeate, respectively. To confirm the membrane fouling of both membranes during the filtration, the observed water uxes were converted to normalized uxes only for the characterization of the NOM retention performance. Furthermore, the retention performances for the pharmaceuticals in the pH range 3–10, and for inorganic salts at concentrations of 1, 5, and 10 mM, were used to evaluate the charge effects between the ceramic_{GO} membrane and the various compounds.

3. RESULTS AND DISCUSSION

3.1. Physicochemical Property of GO Nanosheets.

Yellowish-brown GO powders were prepared in the laboratory using the modified Hummers method, 28 indicating that the graphite (black) was modified chemically by oxygenated functional groups. Because the physicochemical properties of prepared GO powders can affect the membrane modification (fabrication) and performance, we used various analysis techniques to demonstrate the unique morphological and structural properties of the GO powders (Figure 1). Bio-TEM images revealed that the prepared GO powders produced nanosheets of a few layered carbon atoms with lateral sizes of 100-2000 nm (Figure 1a). This is consistent with previous research showing that GO nanosheets exhibit a general tendency to form multilayered carbon agglomerates of several sizes. 16 Addition, the XRD pattern (Figure 1b) of the prepared GO powders had a sharp diffraction peak at a 2θ value of 11.1° , corresponding to the crystal phases of GO particles.

FTIR, XPS, and Raman measurements were used to confirm the physicochemical structure of the GO nanosheets. In the FTIR spectrum (Figure 1c), the GO nanosheets exhibited the usual peak at 1620 cm⁻¹, corresponding to unoxidized sp² C=C bonds. In particular, two large peaks were observed at 1729 and 1379 cm⁻¹, corresponding to carboxyl group stretching vibrations of C-O and C=O bonds, respectively. In addition to the carboxyl group vibrations, two unusual peaks were detected at 1293 and 1039 cm⁻¹, revealing the presence of epoxy and alkoxy groups, respectively. These results are consistent with previous research indicating that the GO nanosheets are functionalized with oxygen-rich groups such as hydroxyl, carboxyl, epoxy, alkoxy, and ether groups.²⁸

Similarly, the oxygen-rich functional groups in GO nanosheets were also observed in XPS spectra, as shown in Figure 1d. While the peak at 284.8 eV is consistent with the unoxidized C-C/C=C/C-H bonds, three peaks were also observed at 286.9, 288.3, and 289.1 eV, which correspond to oxidized C-OH/C-O-C, C=O, and COOH bonds, respectively. Furthermore, the Raman spectrum (Figure 1e) exhibited the oxidized sp² graphitic carbon (G peak at 1600 cm⁻¹) and carbon lattice distortion (D peak at 1350 cm⁻¹) with an I_D/I_G ratio of 1.46. Generally, a larger peak intensity ratio of $I_{\rm D}/I_{\rm G}$ is assigned to increased distortion in the graphitized structure, 31,32 resulting in from a higher proportion of oxygencontaining functional groups in the GO nanosheets. Thus, we consider our functionalized GO nanosheets to be an encouraging material for the modification of intrinsic membrane properties.

3.2. Characterization of Ceramic_{GO} Membranes. To confirm that the functionalized GO nanosheets were coated on the pristine ceramic membranes for different MWCOs, the surface morphology, hydrophobicity, roughness value, and surface charge of pristine and ceramic_{GO} membranes were

ACS Applied Materials & Interfaces

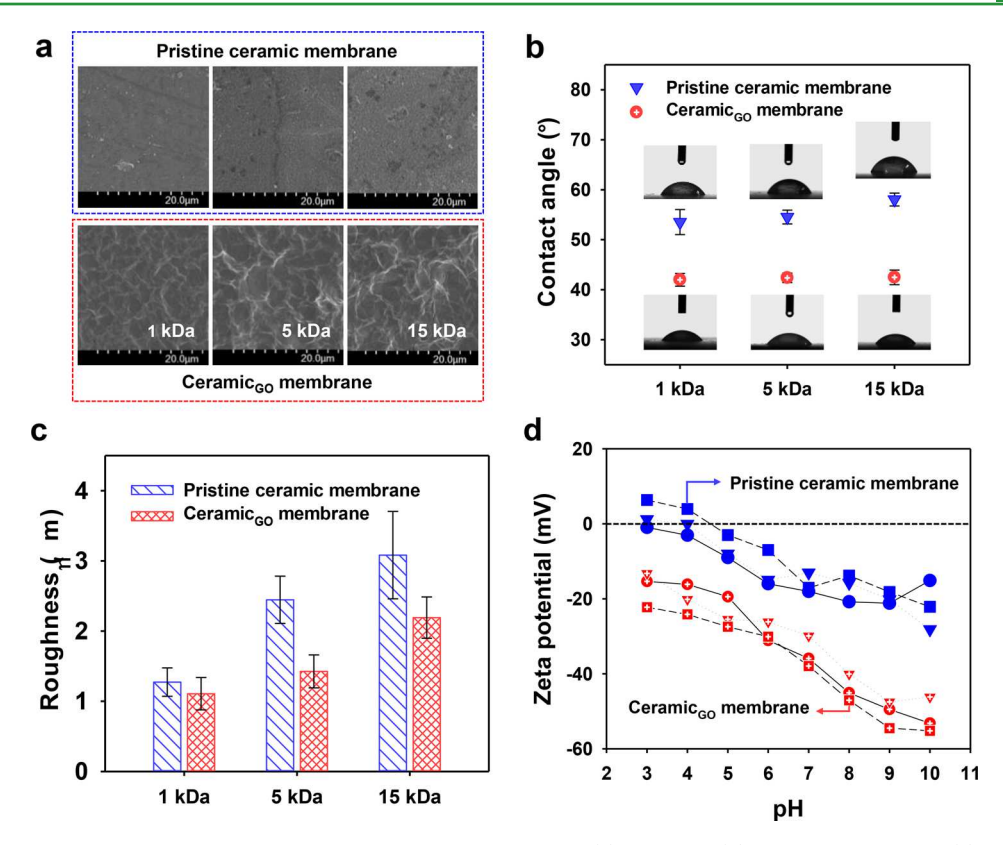


Figure 2. Characteristics of the pristine ceramic and ceramic GO membranes with (a) FE-SEM, (b) water contact angle, (c) CLSM, and (d) zeta potential analysis (nominal MWCOs: 1 kDa = rectangle; 5 kDa = inverted triangle; 10 kDa = circle).

further characterized by FE-SEM, water contact angle, CLSM, and zeta potential measurements, respectively (Figure 2). FE-SEM images (Figure 2a) revealed that the surfaces of ceramic_{GO} membranes were changed significantly to a scale-like structure, while pristine ceramic membranes had relatively clean surfaces. The contact angle experiments (Figure 2b) also indicated that the hydrophilicity of the pristine ceramic membranes (average 55.4°) increased after GO coating (42.3°), due to the extremely hydrophilic properties of GO nanosheets. However, these differences in average contact angles were not significant due to the relatively hydrophilic properties of the pristine ceramic membranes; this is discussed in more detail below in terms of the decreased pure water uxes for ceramic_{GO} membranes. As shown by the roughness values in Figure 2c, the ceramic_{GO} membranes appeared to be significantly smoother than the pristine ceramic membranes. This effect has been observed in previous studies of polyamide and poly(ether sulfone) membranes, where the roughness values decreased after GO coating. 14,26,27 Additionally, the zeta potential measurements (Figure 2d) revealed relatively large negative charge values for the ceramic_{GO} membranes over a wide pH range in comparison to the pristine ceramic membranes.

The results of the comprehensive set of characterization experiments described above demonstrate that the ceramic_{GO} membranes used in this study were successful in providing good coverage of GO nanosheets on the pristine ceramic membrane. The stable GO coating on the pristine ceramic membrane can be explained speculatively by strong hydrogen bonding interactions between the hydroxyl groups on the ceramic membrane surfaces and carboxylic groups in GO nanosheets, as illustrated in Figure 3. The carboxyl group is mainly from oxygen-containing groups in GO nanosheets



Figure 3. Schematics of the ceramic membrane modification with functionalized GO nanosheets.

(Figure 1c,d). Because the hydroxyl groups are usually present on the metal oxide surfaces (i.e., TiO2) of ceramic membranes (Figure S2),³³ a strong interaction between hydroxyl and carboxyl groups is expected for the GO nanosheets coated on the ceramic membrane surfaces (Figure S3). This is presumably because the GO nanosheets are partially ionized with anions of carboxylate and cations of hydrogen, resulting in self-assembled reactions with the hydroxyl groups on metal oxide surfaces during the heat treatment. Thus, the carboxylate anions on the GO nanosheets interact with metal oxides on ceramic membrane surfaces where they then concentrate to form a GO coating, leading to a buildup of negative charge on the ceramic_{GO} membrane surfaces (Figure 2d). Furthermore, the solid-liquid interfacial phenomenon in dispersed GO suspensions results in interactions with hydrophilic metal oxides on ceramic membrane surfaces, leading to the interfacial

enrichment of GO onto the ceramic membrane surface by the self-assembly process, which results in higher hydrophilicities for ceramic_{GO} membranes (Figure 2b).

To determine how functionalized GO nanosheets in uence the intrinsic membrane transport properties, we performed pure water permeability tests for the pristine ceramic and ceramic_{GO} membranes (Figure 4). The pure water permeability

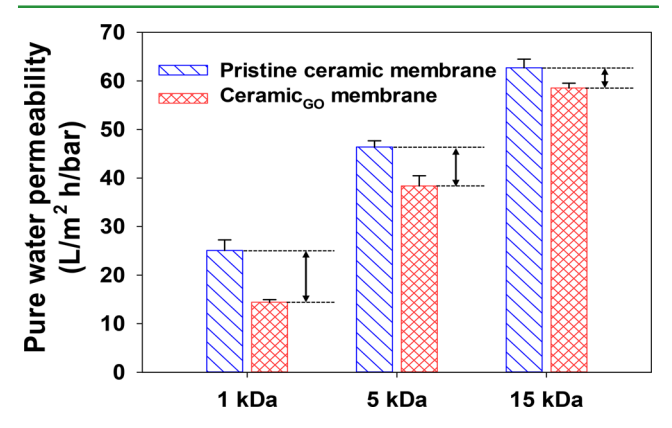


Figure 4. Pure water permeability of the pristine ceramic and ceramic_{GO} membranes with different MOCOs of 1, 5, and 15 kDa. Operating conditions: $\Delta P = 3$ bar; stirring speed = 300 rpm; pH = 7; conductivity = 300 μ S/cm.

of pristine membranes was 25.1 L/m² h/bar for 1 kDa, 46.4 L/ m² h/bar for 5 kDa, and 62.7 L/m² h/bar for 15 kDa, which decreased to 14.4 L/m² h/bar for 1 kDa, 38.4 L/m² h/bar for 5 kDa, and 58.6 L/m² h/bar for 15 kDa after the membranes were coated with GO nanosheets. It is interesting to note that the pure water permeability significantly decreased as the nominal MWCOs of ceramic_{GO} membranes decreased. Our previous studies have shown that the pure water permeability with respect to the MWCOs exhibited similar trends for poly(ether sulfone) membranes after GO coating. 26,27 Although overall GO-coated membranes had higher pure water uxes than the pristine poly(ether sulfone) membranes, the pure water uxes significantly decreased with decreasing MWCOs. These results can be explained in terms of smaller membrane pore sizes caused by the stacked positioning of GO nanosheets on the membranes, resulting in dense GO nanochannels with the excessive enrichment of interfacial GO onto the membrane surfaces. In particular, the hydrophilicity of the supported membrane plays an important role in the formation of GO nanochannels on the membrane, resulting in a trade-off in pure water permeability/ ux between the hydrophilic ceramic and hydrophobic poly(ether sulfone) membranes after GO coating.

3.3. Retention Performance of the Ceramic_{GO} **Membrane.** The water ux behavior described above indicates that water resistance on the ceramic_{GO} membrane could be affected by the formation/positioning (i.e., size and shape) and physicochemical properties of GO nanochannels. To demonstrate the membrane removal mechanisms in these channels, various compounds that may pose serious problems in aquatic environments were used as a single feed in water, under the experimental conditions of pH 7 and a conductivity of 300 μ S/cm. As shown in Figure 5, the pristine ceramic and ceramic_{GO} membranes with a 1 kDa MWCO were examined to evaluate membrane retention performance for four organic compounds (HA, TA, IBP, and SMX) with different molecular sizes and hydrophobicity values and inorganic salts (NaCl, Na₂SO₄,

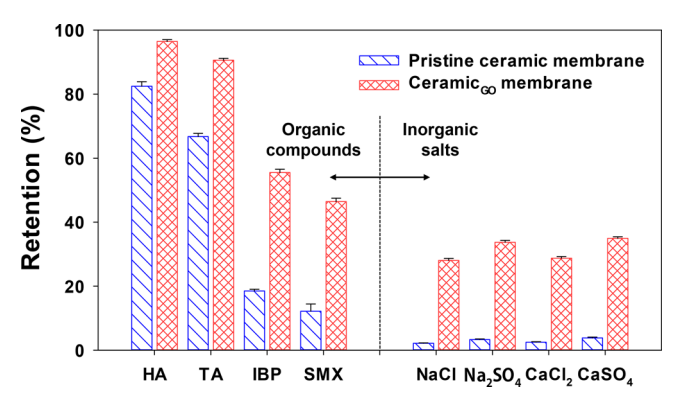


Figure 5. Retention of NOMs (HA and TA), pharmaceuticals (IBP and SMX), and inorganic salts (NaCl, Na₂SO₄, CaCl₂, and CaSO₄) by the pristine ceramic and ceramic_{GO} membranes (MWCO = 1 kDa). Operating conditions: $\Delta P = 3$ bar; stirring speed = 300 rpm; pH = 7; conductivity = 300 μ S/cm; HA and TA = 10 mg/L; IBP and SMX = 10 μ M; NaCl, Na₂SO₄, CaCl₂, and CaSO₄ = 10 mM.

CaCl₂, and CaSO₄) with mixed monovalent and/or divalent ions. The next section discusses the retention and mechanisms for each of these compounds.

3.3.1. NOM Retention. Figure 5 shows the retention of NOM (HA and TA) for the pristine ceramic and ceramic_{GO} membranes. NOM was removed significantly with high yields after filtration by the ceramic_{GO} membrane (96.5% for HA and 90.6% for TA), while the pristine ceramic membrane also achieved reasonable retention rates (82.5% for HA and 66.8% for TA). Although the retention of TA was slightly lower than that of HA due to its smaller molecular size, 27 the mechanisms for the retention of these kinds of NOM in pristine ceramic membranes are mainly size exclusion and hydrophobic adsorption. In addition to these mechanisms, the ceramic_{GO} membrane is also subject to electrostatic repulsion between NOM and negatively charged ceramic_{GO} membrane surfaces. Even though the pristine membrane had a negative charge value (-15.7 mV) at pH 7, the ceramic_{GO} membrane had a higher negative charge value after GO coating (Figure 2d) due to the presence of functionalized GO nanosheets on the membrane.

It must be noted that the adsorption effect of GO nanosheets on the modified membranes should be completely omitted from any analysis of the retention performance of the ceramic_{GO} membrane. Generally, GO is well-known as an appropriate adsorbent for various organic compounds.³⁴ However, in our previous retention tests with HA and TA for GO-coated membranes, the permeate concentrations were stabilized with a low adsorption capacity of GO nanosheets during filtration. ^{26,27} We attributed the high retention of NOM mainly to the defining removal mechanisms (i.e., charge effects and size exclusion). Although the intrinsic capacity of GO adsorption, commonly reached around 1.5 h, also contributed to the retention capability of the membrane, the adsorption effect on the ceramic_{GO} membrane surface should be negligible, because we intentionally stabilized each retention test for at least 3 h prior to collecting samples of feed and permeate solutions for analysis.

Previous studies have suggested that a lack of membrane fouling can be attributed to high roughness and/or hydrophobicity values. The ceramic $_{\rm GO}$ membrane had a lower roughness value than the pristine membrane (Figure 2c), leading to reduced contact opportunities for NOM retention with a decreased membrane surface area. Additionally, the ux

decline trends of ceramic_{GO} membranes were significantly lower than those of pristine ceramic membranes (Figure S4): 4.9% for HA and 14.0% for TA. The ceramic_{GO} membrane exhibited higher hydrophilicity (Figure 2b) than the pristine membrane, leading to reduced hydrophobic attractions between NOM and the membrane surface/pores, resulting in lower ux decline with minimal membrane fouling (Figure S4). Thus, the ceramic_{GO} membrane performed better than the pristine ceramic membrane in terms of NOM retention and ux decline because of its lower roughness and higher hydrophilicity after GO coating.

3.3.2. Pharmaceutical Retention. In contrast to the high retention achieved for the relatively large NOM molecules, retention trends were lower for the small-molecule pharmaceuticals (IBP and SMX) in both pristine ceramic and ceramic_{GO} membranes (Figure 5) under the pH condition of this experiment. The pristine ceramic membrane retained 20% less of these pharmaceuticals. However, the ceramic_{GO} membrane significantly improved retention with values in the range 54.3-56.8% and 45.2-47.8% for IBP and SMX, respectively. We attributed this improved retention for both IBP and SMX to reduced transport in GO nanochannels on the ceramic_{GO} membrane surface. In addition, the retention of IBP by the ceramic_{GO} membrane was slightly higher than that of SMX, because this more hydrophobic compound can be readily adsorbed onto the membrane surface and/or pores.

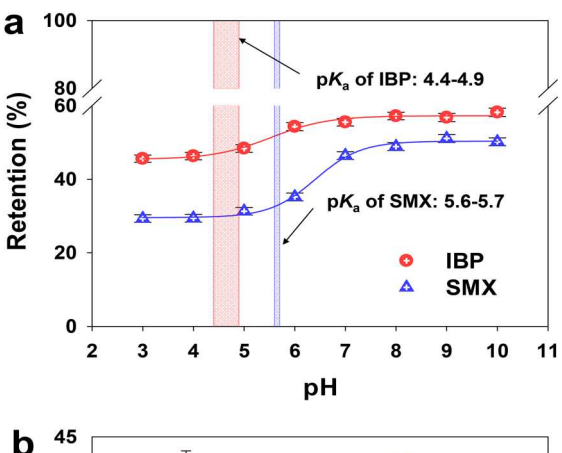
IBP and SMX had significantly different adsorption affinities to the membrane due to their formation of highly charged ions under pH condition of this experiment. SMX has a low adsorption affinity to the pristine membrane due to its relatively low log K_{OW} value (Table 1). Moreover, the relatively high log $K_{\rm OW}$ of IBP (Table 1) is for the neutral species, which are prevalent below the pK_a value, but not under the pH condition of this experiment where the deprotonated species dominated.³⁸ For these reasons, size exclusion and electrostatic interaction (i.e., repulsion) to retention had obvious effects for the ceramic_{GO} membrane during the filtration of pharmaceuticals, compared with the pristine ceramic membrane. In particular, we attribute the retention of pharmaceuticals by the ceramic_{GO} membrane to their size and dissociation behavior under the experimental pH; we discuss this in more detail later, regarding to the effect of pH on the ceramic_{GO} membrane.

3.3.3. Inorganic Salt Retention. The pristine ceramic membrane had almost no retention of inorganic salts (<5%), while the inorganic salt retention significantly increased after GO coating (Figure 5): the retention levels of NaCl, Na₂SO₄, CaCl₂, and CaSO₄ were 28.1%, 33.7%, 28.7%, and 34.9%, respectively. These results indicate that the water retention performance of the ceramic_{GO} membrane depended significantly on the two dominant factors of size exclusion (gaps between GO nanochannels) and charge effects (negative charge between membranes and compounds). On the basis of the retention rates of the different size compounds, the gaps between GO nanochannels were estimated to be at approximately 400 Da (i.e., 1.15 nm). This result is consistent with previous findings: one study found that a GO membrane with an estimated pore size of approximately 1 nm had similar retention trends for NaCl and Na₂SO₄. ¹⁶

In particular, the retention of inorganic salts revealed similar trends with respect to the monovalent (NaCl and CaCl₂) and divalent (Na₂SO₄ and CaSO₄) anions. This can be explained by the fact that every anion must be removed along with one cation in order to satisfy electroneutrality conditions. To

achieve electroneutrality conditions, fewer divalent anions must pass through the membrane, and thus the retention of Na₂SO₄ and CaSO₄ was higher than that of NaCl and CaCl₂. Additionally, in water the divalent anions are in equilibrium with their monovalent counterparts (i.e., HSO₄⁻), leading to more anionic conditions compared to the monovalent anions, which results in increased electrostatic repulsion between the electrolyte anions and the negatively charged ceramic_{GO} membrane.

3.4. E ects of pH and Ionic Strength on the Ceramic_{GO} Membrane. To comprehensively explore the charge effects between membranes and compounds, we confirmed the retention performance with ceramic_{GO} membranes (MWCO = 1 kDa) for the pharmaceuticals (IBP and SMX) under various pH conditions, and the inorganic salts (NaCl, Na₂SO₄, CaCl₂, and CaSO₄) at different solution concentrations (Figure 6). In general, pH conditions can affect



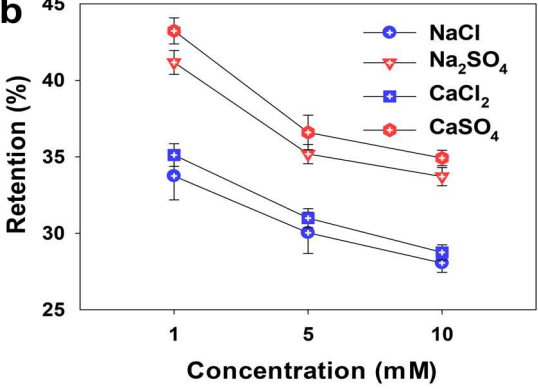


Figure 6. Retention of (a) IBP and SMX at various pH conditions and (b) inorganic salts at different solution concentrations by the ceramic_{GO} membrane (MWCO = 1 kDa). Operating conditions: ΔP = 3 bar; stirring speed = 300 rpm; IBP and SMX = 10 μ M at a pH range of 3-10 and a conductivity of 300 μS/cm; NaCl, Na₂SO₄, $CaCl_2$, and $CaSO_4 = 1$, 5, and 10 mM at pH of 7.

not only the membrane charge but also the physicochemical properties of pharmaceuticals (i.e., hydrophobicity and solubility). In particular, the speciation of both IBP and SMX is a function of pH (Figure S5), thus allowing a systematic investigation of the removal mechanisms for the ceramic_{GO} membrane. Figure 6a represents the retention of IBP and SMX for the ceramic_{GO} membrane over a pH range of 3-10. The retention of IBP and SMX in the ceramic_{GO} membrane decreased significantly as the pH decreased to below their pK_a values because of the conversion of the negative pharmaceutical species to their neutral forms.

Although IBP exhibited slightly higher retention than SMX due to its higher hydrophobicity, both electrostatic repulsion and size exclusion contributed significantly to the retention of the two charged pharmaceuticals in the ceramic_{GO} membrane. Moreover, the retention behaviors of IBP and SMX followed a sigmoidal shape with increasing pH, exhibiting similar trends to their speciation curves (Figure S5). It is interesting to note that the in ection points for these pharmaceuticals were slightly lower than their pK_a values. This phenomenon is consistent with previous work where some retention of the negative species was observed under acidic conditions. 39,40 Because of the passage of protons through the GO nanochannels and/or membrane pores, the local pH could be lower than the feed solution, which to some extent could explain the differences between the in ection points and the pKa values of the pharmaceuticals (Figure 6a).

Figure 6b also represents the retention of NaCl, Na₂SO₄, CaCl₂, and CaSO₄ at solution concentrations of 1, 5, and 10 mM. As the solution concentration (i.e., ionic strength) increased, the retention of inorganic salts decreased significantly. In particular, the divalent anions Na2SO4 and CaSO4 exhibited stronger decreases in retention with ionic strength than the monovalent anions NaCl and CaCl₂. Specifically, the retention of Na2SO4 and CaSO4 decreased significantly from 42.2% at 1 mM to 34.3% at 10 mM, whereas the retention of NaCl and CaCl₂ decreased only slightly from 34.4% at 1 mM to 28.4% at 10 mM. This result can be explained in terms of Debye length effects, which decrease with increasing ionic strength. 16 Additionally, electrostatic repulsion between the inorganic salts and the negatively charged membrane surfaces decreased due to thinning of the electrical double layers, therefore reducing the retention efficiency of inorganic salts in the ceramic_{GO} membrane.

4. CONCLUSIONS

Oxygen-rich functionalized GO nanosheets, produced from pure graphite using the modified Hummer method, were successfully coated onto commercially available ceramic membrane using the vacuum method. Based on their physicochemical properties, we attributed the structure of the modified ceramic_{GO} membranes mainly to hydrogen bond interactions between the hydroxyl groups on the ceramic membrane and the carboxylic GO nanosheets. The ceramic_{GO} membrane was superior to the pristine ceramic membrane for the retention of target NOM, pharmaceuticals, and inorganic salts due to its higher hydrophilicity as well as the buildup of negative charge and decrease of pore size, leading to reduced hydrophobic attraction, strong electrostatic repulsion, and effective size exclusion, thereby improving removal mechanisms for water treatment. Thus, the beneficial effects of the coated GO membrane may qualify it as an excellent and advanced water treatment technology for drinking water and wastewater reclamation fields.

ASSOCIATED CONTENT

S Supporting Information

The Supporting Information is available free of charge on the ACS Publications website at DOI: 10.1021/acsami.7b14217.

Additional information for the schematic illustration of the ceramic_{GO} membrane modification (Figure S1), XRD

pattern of the pristine ceramic membrane (Figure S2), XPS spectra of ceramic $_{\rm GO}$ membrane (Figure S3), normalized ux declines of the pristine ceramic and ceramic $_{\rm GO}$ membranes (Figure S4), and speciation of IBP and SMX (Figure S5) (PDF)

AUTHOR INFORMATION

Corresponding Author

*Phone: 1-803-777-8952. Fax: 1-803-777-0670. E-mail: yoony@cec.sc.edu.

ORCID

Mahdi Fathizadeh: 0000-0002-2349-7406 Yeomin Yoon: 0000-0001-9893-0924

Notes

The authors declare no competing financial interest.

ACKNOWLEDGMENTS

This research was supported by a grant (code 18IFIP-B088091-05) from Industrial Facilities & Infrastructure Research Program funded by Ministry of Land, Infrastructure, and Transport of Korean government. In addition, this research was supported by the U.S. National Science Foundation (OIA-1632824).

REFERENCES

- (1) Cho, J.; Amy, G.; Pellegrino, J. Membrane Filtration of Natural Organic Matter: Initial Comparison of Rejection and Flux Decline Characteristics with Ultrafiltration and Nanofiltration Membranes. *Water Res.* **1999**, 33 (11), 2517–2526.
- (2) Kiso, Y.; Nishimura, Y.; Kitao, T.; Nishimura, K. Rejection Properties of Non-phenylic Pesticides with Nanofiltration Membranes. *J. Membr. Sci.* **2000**, *171* (2), 229–237.
- (3) Kiso, Y.; Sugiura, Y.; Kitao, T.; Nishimura, K. Effects of Hydrophobicity and Molecular Size on Rejection of Aromatic Pesticides with Nanofiltration Membranes. *J. Membr. Sci.* **2001**, *192* (1-2), 1–10.
- (4) Yoon, Y.; Westerhoff, P.; Snyder, S. A.; Wert, E. C. Nanofiltration and Ultrafiltration of Endocrine Disrupting Compounds, Pharmaceuticals and Personal Care Products. *J. Membr. Sci.* **2006**, 270 (1), 88–100
- (5) Yoon, Y.; Westerhoff, P.; Snyder, S. A.; Wert, E. C.; Yoon, J. Removal of Endocrine Disrupting Compounds and Pharmaceuticals by Nanofiltration and Ultrafiltration Membranes. *Desalination* **2007**, 202 (1), 16–23.
- (6) Berg, P.; Hagmeyer, G.; Gimbel, R. Removal of Pesticides and Other Micropollutants by Nanofiltration. *Desalination* **1997**, *113* (2–3), 205–208.
- (7) Boussahel, R.; Bouland, S.; Moussaoui, K.; Montiel, A. Removal of Pesticide Residues in Water Using the Nanofiltration Process. *Desalination* **2000**, *132* (1–3), 205–209.
- (8) Chen, X.; Mao, S. S. Titanium Dioxide Nanomaterials: Synthesis, Properties, Modifications, and Applications. *Chem. Rev.* **2007**, *107* (7), 2891–2959.
- (9) Huang, S.-Y.; Ganesan, P.; Park, S.; Popov, B. N. Development of a Titanium Dioxide-Supported Platinum Catalyst with Ultrahigh Stability for Polymer Electrolyte Membrane Fuel Cell Applications. *J. Am. Chem. Soc.* **2009**, *131* (39), 13898–13899.
- (10) Reddy, K. R.; Hassan, M.; Gomes, V. G. Hybrid Nanostructures Based on Titanium Dioxide for Enhanced Photocatalysis. *Appl. Catal., A* **2015**, *489*, 1–16.
- (11) Celik, E.; Park, H.; Choi, H.; Choi, H. Carbon Nanotube Blended Polyethersulfone Membranes for Fouling Control in Water Treatment. *Water Res.* **2011**, *45* (1), 274–282.

- (12) Lekawa-Raus, A.; Walczak, K.; Kozlowski, G.; Wozniak, M.; Hopkins, S. C.; Koziol, K. K. Resistance—Temperature Dependence in Carbon Nanotube Fibres. *Carbon* **2015**, *84*, 118–123.
- (13) Zhang, J.; Xu, Z.; Mai, W.; Min, C.; Zhou, B.; Shan, M.; Li, Y.; Yang, C.; Wang, Z.; Qian, X. Improved Hydrophilicity, Permeability, Antifouling and Mechanical Performance of PVDF Composite Ultrafiltration Membranes Tailored by Oxidized Low-dimensional Carbon Nanomaterials. *J. Mater. Chem. A* **2013**, *1* (9), 3101–3111.
- (14) Choi, W.; Choi, J.; Bang, J.; Lee, J.-H. Layer-by-Layer Assembly of Graphene Oxide Nanosheets on Polyamide Membranes for Durable Reverse-Osmosis Applications. *ACS Appl. Mater. Interfaces* **2013**, 5 (23), 12510–12519.
- (15) Han, Y.; Xu, Z.; Gao, C. Ultrathin Graphene Nanofiltration Membrane for Water Purification. *Adv. Funct. Mater.* **2013**, 23 (29), 3693–3700.
- (16) Hu, M.; Mi, B. Enabling Graphene Oxide Nanosheets as Water Separation Membranes. *Environ. Sci. Technol.* **2013**, 47 (8), 3715–3723.
- (17) Joshi, R.; Carbone, P.; Wang, F.-C.; Kravets, V. G.; Su, Y.; Grigorieva, I. V.; Wu, H.; Geim, A. K.; Nair, R. R. Precise and Ultrafast Molecular Sieving through Graphene Oxide Membranes. *Science* **2014**, 343 (6172), 752–754.
- (18) Han, Y.; Jiang, Y.; Gao, C. High-Flux Graphene Oxide Nanofiltration Membrane Intercalated by Carbon Nanotubes. *ACS Appl. Mater. Interfaces* **2015**, *7* (15), 8147–8155.
- (19) Mi, B. Graphene Oxide Membranes for Ionic and Molecular Sieving. *Science* **2014**, 343 (6172), 740–742.
- (20) Zinadini, S.; Zinatizadeh, A. A.; Rahimi, M.; Vatanpour, V.; Zangeneh, H. Preparation of a Novel Antifouling Mixed Matrix PES Membrane by Embedding Graphene Oxide Nanoplates. *J. Membr. Sci.* **2014**, *453*, 292–301.
- (21) Chang, Q.; Zhou, J.-e.; Wang, Y.; Liang, J.; Zhang, X.; Cerneaux, S.; Wang, X.; Zhu, Z.; Dong, Y. Application of Ceramic Microfiltration Membrane Modified by Nano-TiO2 Coating in Separation of a Stable Oil-in-Water Emulsion. *J. Membr. Sci.* **2014**, *456*, 128–133.
- (22) Howarter, J. A.; Youngblood, J. P. Amphiphile Grafted Membranes for the Separation of Oil-in-Water Dispersions. *J. Colloid Interface Sci.* **2009**, 329 (1), 127–132.
- (23) Zhou, J.-e.; Chang, Q.; Wang, Y.; Wang, J.; Meng, G. Separation of Stable Oil–Water Emulsion by the Hydrophilic Nano-Sized ZrO2Modified Al2O3Microfiltration Membrane. *Sep. Purif. Technol.* **2010**, 75 (3), 243–248.
- (24) Hu, X.; Yu, Y.; Zhou, J.; Wang, Y.; Liang, J.; Zhang, X.; Chang, Q.; Song, L. The Improved Oil/Water Separation Performance of Graphene Oxide Modified Al2O3Microfiltration Membrane. *J. Membr. Sci.* **2015**, 476, 200–204.
- (25) Zhong, J.; Sun, X.; Wang, C. Treatment of Oily Wastewater Produced from Refinery Processes Using Flocculation and Ceramic Membrane Filtration. Sep. Purif. Technol. 2003, 32 (1), 93–98.
- (26) Chu, K. H.; Huang, Y.; Yu, M.; Heo, J.; Flora, J. R.; Jang, A.; Jang, M.; Jung, C.; Park, C. M.; Kim, D.-H.; Yoon, Y. Evaluation of Graphene Oxide-Coated Ultrafiltration Membranes for Humic Acid Removal at Different pH and Conductivity Conditions. *Sep. Purif. Technol.* **2017**, *181*, 139–147.
- (27) Chu, K. H.; Huang, Y.; Yu, M.; Her, N.; Flora, J. R.; Park, C. M.; Kim, S.; Cho, J.; Yoon, Y. Evaluation of Humic Acid and Tannic Acid Fouling in Graphene Oxide-coated Ultrafiltration Membranes. ACS Appl. Mater. Interfaces 2016, 8 (34), 22270–22279.
- (28) Marcano, D. C.; Kosynkin, D. V.; Berlin, J. M.; Sinitskii, A.; Sun, Z.; Slesarev, A.; Alemany, L. B.; Lu, W.; Tour, J. M. Improved Synthesis of Graphene Oxide. ACS Nano 2010, 4 (8), 4806–4814.
- (29) Li, H.; Song, Z.; Zhang, X.; Huang, Y.; Li, S.; Mao, Y.; Ploehn, H. J.; Bao, Y.; Yu, M. Ultrathin, Molecular-sieving Graphene Oxide Membranes for Selective Hydrogen Separation. *Science* **2013**, 342 (6154), 95–98.
- (30) Song, J. J.; Huang, Y.; Nam, S.-W.; Yu, M.; Heo, J.; Her, N.; Flora, J. R.; Yoon, Y. Ultrathin Graphene Oxide Membranes for the Removal of Humic Acid. Sep. Purif. Technol. 2015, 144, 162–167.

- (31) Ferrari, A. C.; Robertson, J. Interpretation of Raman Spectra of Disordered and Amorphous Carbon. *Phys. Rev. B: Condens. Matter Mater. Phys.* **2000**, *61* (20), 14095.
- (32) Graf, D.; Molitor, F.; Ensslin, K.; Stampfer, C.; Jungen, A.; Hierold, C.; Wirtz, L. Spatially Resolved Raman Spectroscopy of Single-and Few-layer Graphene. *Nano Lett.* **2007**, *7* (2), 238–242.
- (33) Alami Younssi, S.; Iraqi, A.; Rafiq, M.; Persin, M.; Larbot, A.; Sarrazin, J. γ Alumina Membranes Grafting by Organosilanes and Its Application to the Separation of Solvent Mixtures by Pervaporation. *Sep. Purif. Technol.* **2003**, 32 (1-3), 175–179.
- (34) Ai, L.; Zhang, C.; Chen, Z. Removal of Methylene Blue from Aqueous Solution by a Solvothermal-synthesized Graphene/Magnetite Composite. J. Hazard. Mater. 2011, 192 (3), 1515–1524.
- (35) Ghosh, A. K.; Jeong, B.-H.; Huang, X.; Hoek, E. M. Impacts of Reaction and Curing Conditions on Polyamide Composite Reverse Osmosis Membrane Properties. *J. Membr. Sci.* **2008**, *311* (1), 34–45.
- (36) Ho, C.-C.; Zydney, A. L. Effect of Membrane Morphology on the Initial Rate of Protein Fouling During Microfiltration. *J. Membr. Sci.* 1999, 155 (2), 261–275.
- (37) Vrijenhoek, E. M.; Hong, S.; Elimelech, M. Influence of Membrane Surface Properties on Initial Rate of Colloidal Fouling of Reverse Osmosis and Nanofiltration Membranes. *J. Membr. Sci.* **2001**, 188 (1), 115–128.
- (38) Nghiem, L. D.; Schäfer, A. I.; Elimelech, M. Pharmaceutical Retention Mechanisms by Nanofiltration Membranes. *Environ. Sci. Technol.* **2005**, 39 (19), 7698–7705.
- (39) Childress, A. E.; Elimelech, M. Relating Nanofiltration Membrane Performance to Membrane Charge (Electrokinetic) Characteristics. *Environ. Sci. Technol.* **2000**, 34 (17), 3710–3716.
- (40) Tanninen, J.; Nyström, M. Separation of Ions in Acidic Conditions Using NF. *Desalination* **2002**, *147* (1–3), 295–299.
- (41) Geankoplis, C. J. Transport Processes and Unit Operations, 3rd ed.; Prentice-Hall: Sydney, Australia, 1993.
- (42) Avdeef, A.; Berger, C. M.; Brownell, C. pH-metric Solubility. 2: Correlation between the Acid-base Titration and the Saturation Shake-flask Solubility-pH Methods. *Pharm. Res.* **2000**, *17* (1), 85–89.
- (43) Hansch, C.; Sammes, P. G.; Taylor, J. B. Comprehensive Medicinal Chemistry: The Rational Design, Mechanistic Study & Therapeutic Applications of Chemical Compounds; Pergamon Press: New York, 1989; Vol. 6.
- (44) Lucida, H.; Parkin, J.; Sunderland, V. Kinetic Study of the Reaction of Sulfamethoxazole and Glucose under Acidic Conditions: I. Effect of pH and Temperature. *Int. J. Pharm.* **2000**, *202* (1), 47–62.
- (45) Budavari, S. *Merck Index*, 12th ed.; Merck & Co Inc.: Whitehouse Station, NJ, 1996.